



Cite this: *Sustainable Food Technol.*, 2023, 1, 590

## Study on drying kinetics, antioxidant activity, total bioactive compounds, physicochemical properties and microstructural characteristics of dehydrated star fruits (*Averrhoa carambola*) by different drying methods†

Jayanti Dhara, Suman kumar Saha, Madhumita Saha and Runu Chakraborty\*

Drying ensures an uninterrupted supply of highly perishable and seasonal fruits such as star fruit (*Averrhoa carambola*). In this study, the effect of different drying methods-hot air drying (HAD), freeze drying (FD) and microwave drying (MWD; 100, 450 and 800 W) on drying kinetics, antioxidant content, physicochemical properties and surface microstructure properties of star fruits was thoroughly investigated. Among seven different thin-layer drying models, the two-term model is the best-fitted model with the lowest SSE (0.00358–0.000058) value. The FD sample exhibited the least deviation in textural attributes from fresh samples, as a low temperature and pressure gradient maintained the smooth, granular and porous structure of fresh fruits. In contrast, high temperature dried star fruits demonstrated a hard and brittle structure with low resilience and adhesiveness due to the fast moisture removal process and high pressure gradient during drying. High temperature dried products also exhibited a darker color characteristic of phenolic degradation products than the FD sample. Among all dried samples, the HAD star-fruit possessed a higher total phenolic content ( $1139.67 \pm 4.07$  mg GAE/100 g dm) and total flavonoid content ( $4.71 \pm 0.05$  mg QE/100 g dm), DPPH (95% inhibition) and FRAP (ferric reducing antioxidant potential) radical scavenging activity ( $148.52 \pm 0.05$   $\mu\text{mol g}^{-1}$ ) as well as the highest content of chlorogenic acid ( $79.34 \pm 2.38$  mg/100 g), gallic acid ( $15.13 \pm 0.45$  mg/100 g), kaempferol ( $48.85 \pm 1.46$  mg/100 g), myricetin ( $106.38 \pm 3.19$  mg/100 g), and *trans*-cinnamic acid ( $186.85 \pm 5.60$  mg/100 g). The HAD method was adjudged to be the best drying technique for star fruits.

Received 8th February 2023  
Accepted 7th June 2023

DOI: 10.1039/d3fb00024a  
[rsc.li/susfoodtech](http://rsc.li/susfoodtech)

### Sustainability spotlight

Drying can significantly improve sustainability by extending the shelf life of perishable fruits and vegetables, reducing food waste, lowering the need for energy-intensive transportation and storage methods, and preserving surplus production during peak harvest season. Sun drying is preferred for fruits, but instrument-based highly energy-intensive techniques like hot air drying (HAD), freeze drying (FD) and microwave drying (MWD) are used to yield a final product with desirable characteristics and a shorter processing time. Dried fruits have been extensively used as a source of vitamins, antioxidants, fibres and other key nutrients in different products.

## Introduction

Star fruit (*Averrhoa carambola*) is a star-shaped tropical fruit of the Oxalidaceae family and is primarily used for preparing jam, jelly, desserts, salads and drinks.<sup>1</sup> Being rich in fibres, antioxidants, organic acids, vitamins and minerals, the fruit has been found to be beneficial in preventing several health issues including hypoglycaemia, hypocholesterolaemia, acute liver

damage and diabetes mellitus II.<sup>2,3</sup> Although the fruit holds great commercial potential, losses of up to 50% of the total production can occur in developing countries in Asia and South America due to high perishability and moisture content and the absence of suitable post-harvest procedures.<sup>4</sup>

Previously, the drying process, a popular food processing technique, has been extensively utilized to extend the shelf life of highly perishable food such as fruits and vegetables and ensure the year-long availability of seasonal foods.<sup>5</sup> Drying can significantly improve sustainability in several ways. First, it extends the shelf life of perishable fruits and vegetables, reducing food waste. By removing the moisture content, the process inhibits the growth of spoilage organisms, allowing

Department of Food Technology and Biochemical Engineering, Jadavpur University, Kolkata, India. E-mail: [crunu@hotmail.com](mailto:crunu@hotmail.com)

† Electronic supplementary information (ESI) available. See DOI: <https://doi.org/10.1039/d3fb00024a>



dried fruits and vegetables to be stored for a long time without the need for preservatives or refrigeration. This minimizes the food waste and environmental impact of discarded waste.<sup>6</sup> Additionally, drying lowers the need for energy-intensive transportation and storage methods, as dried products are lightweight and take up lower space than fresh products. This can lower greenhouse gas emissions associated with transportation and refrigeration, thus contributing to sustainability effects. Finally, drying preserves surplus production during peak harvest season, preventing it from going to waste and promoting sustainable agricultural practices. Overall, drying improves sustainability by reducing food waste, minimizing energy requirements and promoting efficient resource utilization in the food supply chain.<sup>7</sup> Sun drying is preferred for fruits, but the weather dependence and susceptibility to contamination necessitates the application of instrument-based highly energy-intensive techniques like hot air drying (HAD), freeze drying (FD) and microwave drying (MWD) for yielding a final product with desirable characteristics and a shorter processing time.<sup>8–10</sup> Dried fruits have been extensively used as a prominent source of vitamins, antioxidants, fibres and other key nutrients in different recipes including fortification and enrichment of food.<sup>11</sup>

Although there is a wealth of information in the literature about the effects of various drying processes on various fruits and vegetables, no data are available on the drying kinetics, physiological properties and product qualities of different drying methods for star fruits. Hence the aim of this study was to evaluate the effects of different drying methods namely HAD, MWD and FD on kinetics, antioxidant activity and different physicochemical attributes of star fruits with raw fruit as the control to identify the most suitable drying method in terms of drying efficiency, quality of final products and cost-effectiveness, and optimize different parameters and surface microstructure characteristics with SEM.

## Materials and methods

### Fruits and chemicals

Fresh star-fruit samples were bought at the local Municipal market in Jadavpur, Kolkata, in February 2022 and were refrigerated within 30 minutes in a freezer at  $-53\text{ }^\circ\text{C}$  (C340-86; New Brunswick Scientific, England, UK) for around 3–5 days. Before refrigeration, the samples were thoroughly rinsed in potable water. Before experimentation, the fruit samples were brought out from the freezer, and kept in an airtight container for two hours to bring their temperature to the ambient.

HPLC-grade water was bought from Sigma-Aldrich (Mumbai, India), and deionized water was obtained from a Milli-Q  $\text{H}_2\text{O}$  purification system (Millipore, MA, USA). Other reagents and solvents were of analytical grade, so they did not require purification before usage. All HPLC and analytical grade solvents and reagents were purchased from Sigma-Aldrich (Mumbai, India) unless otherwise mentioned.

**Sample preparation.** Before experimentation, the fruits were thoroughly rinsed in potable water and then sliced into slabs of 4 mm diameter  $\times$  8 mm width ( $L$ ). 100 g of fresh fruit samples

were used for each drying procedure. 100 g of star fruit was used for each drying process – MWD, HAD and FD, Petri dishes (Borosilicate, Glassco, Kolkata, 150  $\times$  20 mm) were used for the entire drying process.

**Drying procedure.** (1) Microwave drying (MD) was performed in a microwave (Samsung, model no. CE1041DFB, Mumbai, India) with a 2450 MHz operating frequency and variable power levels between 100 and 900 W. For this experiment, three distinct power levels 100, 450 and 800 W, were selected (Fig. 2).

(2) Hot air drying (HAD) was performed at  $70\text{ }^\circ\text{C}$  in a hot air oven (Bionics, model no. BST/HAO-1122, Delhi, India) at  $1\text{ m s}^{-1}$  constant air velocity (Fig. 2).

(3) Freeze drying (FD) was conducted at  $-45\text{ }^\circ\text{C}$  temperature and 0.1 mbar pressure in a lyophilizer (FDU 1200; EYELA, Tokyo, Japan) with a vacuum pressure of 14 Pa, cold trap temperature of  $-45\text{ }^\circ\text{C}$ , heating plate temperature of  $-25\text{ }^\circ\text{C}$ , and condenser temperature of  $-65\text{ }^\circ\text{C}$ . The freeze dried star fruit was pulverized using a mixer grinder (model no. 750, Prestige, Bangalore, India), sieved through a 60 BSS mesh and used for further analysis (Fig. 2).

### Mathematical calculations

**Moisture ratio.** The moisture content was determined using eqn (1)

$$\text{Moisture content (M, wb)} = \frac{W_t - W_d}{W_t} \times 100\% \quad (1)$$

where  $W_t$  and  $W_d$  are the weight of star fruits at a time,  $t$  and  $\infty$  (dry weight).

The moisture content was determined following the AOAC method (AOAC 1990). Drying processes were continuously monitored from the initial moisture content of 11.50 kg water/kg DM (dry matter) to the final moisture content of 0.125 kg water/kg DM.

MR is determined by using eqn (2).

$$\text{MR} = \frac{M_t - M_e}{M_o - M_e}$$

where  $M_t$ ,  $M_o$ ,  $M_e$  are the moisture content of star fruits at time  $= t$ , 0, and  $\infty$  (equilibrium moisture content). Ignoring the  $M_e$ , the equation is reduced to

$$\text{MR} = \frac{M_t}{M_e} \quad (2)$$

**Moisture diffusivity.** Fick's diffusion equation was used to calculate the effective diffusivity of star fruit samples (eqn (3)). Because the fruits were dried after slicing, the samples were presumed to have a slab geometry for this investigation. In all dimensions, shrinkage is considered to be equal. Fick's diffusion equation, which is used to calculate effective diffusivity, is as follows:<sup>12</sup>

$$\text{MR} = \frac{8}{\pi^2} \exp\left(-\frac{\pi^2 D_{\text{eff}} t}{L^2}\right) \quad (3)$$

where MR denotes the dimensionless moisture ratio;  $D_{\text{eff}}$  denotes the effective moisture diffusivity ( $\text{m}^2 \text{ s}^{-1}$ );  $t$  denotes the time in sec;  $L$  denotes the thickness of the samples in  $\text{m}$ .

**Mathematical modelling of drying kinetics.** Seven mathematical models were analysed for effective modelling of different drying methods for star fruits. The models were used to evaluate the impact of the drying period, temperature, and drying methods on drying kinetics (eqn (6)–(12) given in Table 1), or in other words, for effective modelling of the drying properties of star fruits. The experimental drying data were fitted using seven different drying models. The root mean square error (RMSE) was compared to choose the model that gave the best fit for the data. Whereas  $n$ ,  $a$ ,  $b$ ,  $h$ ,  $c$ , and  $g$  are the drying coefficients, whose values vary depending on the model,  $t$  is the drying period (s),  $k$  is the drying constant ( $s^{-1}$ ) and MR is the moisture ratio.

To assess the closeness of fit for the model curves, statistical factors such as root mean squared error (RMSE) (eqn (4)), sum square error (SSE) (eqn (5)) and reduced chi-square were employed.

$$RMSE = \sqrt{\frac{\sum_{i=1}^N (x_i - \hat{x}_i)^2}{N}} \quad (4)$$

where  $i$  = variable  $i$ ;  $N$  = number of non-missing data points;  $x_i$  = actual observation time series;  $\hat{x}_i$  = estimated time series

$$SSE = \frac{1}{n} \left( \sum_{i=1}^n (MR_i^{\text{pred}} - MR_i^{\text{exp}})^2 \right) \quad (5)$$

where  $n$  = number of observations;  $MR_i^{\text{pred}}$  = predicted MR;  $MR_i^{\text{exp}}$  = experimental value of the MR.

**Color measurement.** The color measurement was performed by the following procedure described by Saha *et al.* (2019) using Hunter Lab color measuring equipment (Colour Flex 45/0; Hunter Associates Laboratory, Reston) with a cylindrical optically transparent glass cup. The sample glass cup was filled with raw samples as a control or dried powder, and a black cup was placed above it to keep off the external light. The color of the samples was measured through a sample cup. Color values were determined in the CIE,  $L^*a^*b^*$  space for 10° standard observers and the D65 standard illuminant. The results were expressed in terms of  $L^*$  (lightness = 100 means white and 0 means black),  $a^*$  (redness = – [greenness] to + [redness]), and  $b^*$  (yellowness = – [blue] to + [yellow]) values.  $\Delta E^*$  was expressed as the total color differences of fresh star fruit and dried star fruit samples. Chroma ( $C^*$ ) was used as a quantitative measure of color intensity to assess how different a hue is from a grey color of the

same brightness. The difference between a color and grey color was defined using the hue angle ( $H^*$ ).<sup>13</sup>

$$\Delta E^* = \sqrt{(L_0^* - L_i^*)^2 + (a_0^* - a_i^*)^2 + (b_0^* - b_i^*)^2} \quad (13)$$

$$(H^*) = \tan^{-1}(b^*/a^*) \quad (14)$$

$$\text{Chroma } (C^*) = (a^2 + b^2)^{1/2} \quad (15)$$

where subscript 0 refers to star fruits as are fruit samples. Larger  $\Delta E^*$  denotes a greater change from the reference material of the fresh star fruits.

**Texture analysis.** The texture of the samples was evaluated using a texture profile analyser (Model no: TA. XT Express, Stable Micro Systems, Surrey, UK). The standard double compression texture profile analysis test was performed to estimate the mechanical properties (hardness, fracturability, springiness, gumminess, chewiness, cohesiveness, and resilience) of fresh and dried samples. The instrument was calibrated with 10 kg of force, and a P/5 cylindrical probe (5 mm diameter) at 1 mm  $s^{-1}$  of pre-test speed, trigger force (5 g), compression pressure (75%), waiting time (0  $s^{-1}$ ), test speed (5 mm  $s^{-1}$ ), and post-test speed (5 mm  $s^{-1}$ ).

**Bulk density.** The bulk density of dried powder samples was determined according to the procedure described by Ridgway & Gane.<sup>14</sup> Weighing a predetermined amount of the sample in a 10 ml measuring cylinder allowed us to determine the bulk density of fresh and dried star fruit powder. By dividing the mass of the powder weighed by the volume occupied in the cylinder (in  $g \text{ ml}^{-1}$ ), the bulk density was obtained. The unit of bulk density is expressed as  $\text{kg m}^{-3}$ .

**Extraction and analysis of antioxidants.** Ultrasound-assisted extraction (UAE) of dried samples (1 g powder) of star fruits using a methanol–water binary mixture (50% v/v) (30 : 1 ml g<sup>-1</sup> dry powder) was performed at 70 °C for 1 h in an ultrasonic water bath (*trans-o-sonic*, model no-D150 IH, Mumbai, India). After centrifugation at 4293  $\times g$  for 10 min at 4 °C, the supernatant was filtered using Whatman No. 1 filter paper. The extracts were transferred to a glass tube for further analysis. For HPLC analysis, HPLC grade solvents were used and extracts were filtered by using a syringe filter (P/N: S25N22, 25 mm, 0.22  $\mu$ , Nylon).

#### Estimation of antioxidant content and activities

**Total phenolic content (TPC).** TPC was determined by following the modified protocol of Sarkar *et al.* (2021).<sup>15</sup> Distilled water (1.8 ml) and 0.2 ml of Folin Ciocalteu reagent was added to 0.2 ml of extracted samples. Then, 2 ml (7%) sodium carbonate solution and 0.8 ml distilled water were added. After incubation for 90 minutes in a dark place, the absorbance was recorded at 750 nm using a UV-vis spectrophotometer (Orion Aquamate 8000, Thermos Fisher Scientific, India). Gallic acid was used for the standard curve of the total phenolic content and the results were expressed as mg of gallic acid equivalents (GAE) per 100 g of dry weight of the sample.

**Total flavonoid content (TFC).** TFC was determined using the following modified protocol of Sarkar *et al.* (2021).<sup>15</sup> 1 ml

Table 1 List of seven thin-layer drying models evaluated in this study

Models	Equations	Ref.	Equation no.
Lewis	MR = $\exp(-kt)$	49	(6)
Page	MR = $\exp(-kt^n)$	50	(7)
Modified page	MR = $\exp(-kt)^n$	51	(8)
Logarithmic	MR = $a \exp(-kt) + c$	52	(9)
Henderson Pabis	MR = $a \exp(-kt)$	53	(10)
Two-term	MR = $a \exp(-kt) + b \exp(-gt)$	54	(11)
Wang and Singh	MR = $1 + at + bt^2$	55	(12)



sample was diluted with 4 ml distilled water and to it 0.3 ml 5% (w/v)  $\text{NaNO}_2$  was added. After 5 minutes, 0.3 ml of (10% w/v)  $\text{AlCl}_3$  was added and mixed well. After 6 minutes, 2 ml of 1 M NaOH was added, and the volume was made up to 10 ml immediately by the addition of 2.4 ml of distilled water. The solution was mixed vigorously, and the absorbance was measured by using a UV-vis spectrophotometer at 510 nm after 25 minutes. The standard curve of TFC was obtained using catechin. The result was expressed as mg of catechin equivalents (CAE) per 100 g of dry weight of the sample.

**DPPH (2,2-diphenyl-1-picrylhydrazyl) radical scavenging activity.** DPPH radical scavenging activity of the samples was determined following the modified protocol of S. Ray *et al.* (2017).<sup>13</sup> 2 mg of DPPH was taken and was mixed with 50 ml of methanol in a volumetric flask, and was kept under dark cold conditions. Then, 0.1 ml of the sample was taken in a test tube and mixed with 3.9 ml of DPPH solution. Then, it was incubated in a dark cabinet for 45 min and the absorbance was measured using a UV-vis spectrophotometer at 515 nm. Antioxidant activity was calculated as:

$$\text{Total antioxidant activity (\%)} = \frac{[(\text{control} - \text{sample})/\text{control}]}{100} \quad (16)$$

**Ferric reducing antioxidant potential (FRAP).** FRAP activity of the samples were determined following the modified protocol of S. Ray *et al.* (2017).<sup>13</sup> Phosphate buffer (2.5 ml, 0.2 M, pH 6.6) and 2.5 ml of 1% potassium ferricyanide were added to the sample extract. For 20 minutes, the mixture was incubated at 50 °C. 2.5 ml of 10% trichloroacetic acid was added after incubation, and the mixture was centrifuged at 604×g for 10 minutes. 0.5 ml of 0.1% ferric chloride and 2.5 ml of distilled water were added to the upper layer of the solution. At 700 nm, the resultant mixture's absorbance was determined. The ascorbic acid calibration curve was used to calculate the antioxidant activity. The results were given in units of moles of ascorbic acid equivalent per g.

**HPLC analysis.** HPLC (high-performance liquid chromatography) assay of phenolic compounds was performed following the procedure described by Saha *et al.* (2019).<sup>16</sup> The phenolic profile was analysed by HPLC using an Alliance 2695 HPLC system (Alliance, Water Corporation, Massachusetts, US) coupled with a dual binary pump (model no: 515) and C-18 reversed-phase column (5  $\mu\text{m}$ , 250 mm × 4.6 mm length, USA). Mobile phase A was 0.5 (% v/v) phosphoric acid and B was 90 (% v/v) acetonitrile. The gradient elution was A 100% and B 0% for 0 min, A 100% and B 0% at 2 min, A 80% and B 20% for 2.5 min, A 80% and B 20% at 5 min, A 70% and B 30% at 5.5 min, A 70% and B 30% at 10 min, A 80% and B 20% at 10.5 min, A 80% and B 20% at 12 min, A 100% and B 0% at 12.5 min, and A 100% and B 0% at 15 min. The detection wavelength was 280 nm and the injection volume was 100  $\mu\text{L}$ . The column's temperature was 25 °C and the flow rate was 1  $\text{ml min}^{-1}$ . The contents of various phenolics and extracts were separated at baselines. The individual phenolic content was

evaluated utilizing standard curves and the findings were presented in mg/100 g of extract.

**Scanning electron microscopy (SEM) observation.** The surface microstructure of dried star fruit powder was estimated by using a scanning electron microscope (SEM, INSPECT F50) with an acceleration potential of 5 kV at 2400× magnification. The powder was taken in small amounts on double-sided adhesive tape prepared on aluminium stubs and coated with a 25 nm gold layer at a voltage of 10 kV, 3  $\mu\text{m}$  spot size and 12 mm working distance.<sup>17</sup>

**Statistical analysis.** Minitab 17 was used to statistically assess the effects of drying on color, phenolic content, antioxidant scavenging activity, and FRAP reported in the analytical section. All experiments were performed in triplicate and the results were represented as mean ( $n = 3$ ) and standard deviation ( $\pm$ ). Significant differences at  $p < 0.05$  were determined using one-way ANOVA analysis and Tukey's tests.

## Results and discussion

### Effect of different drying kinetics on star fruits

The drying curves of MR *versus* drying time are shown in Fig. 1.

### Drying efficiency

According to the existing literature, moisture removal is initially rapid because of the rapid evaporation of surface moisture but slows down considerably during the later stage as the moisture diffuses slowly from the inner part to the surface. The drying of star fruit took place from the initial moisture content of 11.50 g moisture/g dm to an equilibrium moisture content of 0.125 g moisture/g dm. For the drying of star fruits, both the constant-rate drying period (CRDP) and the falling rate drying period (FRDP) are present, but the length of both periods depends on the drying techniques. The CRDP was short for faster drying methods – MD<sub>800</sub> and MD<sub>450</sub>, whereas for slower methods like HAD and FD, the CRDP constitutes almost 50–80% of the total drying time. From experimental data for freeze drying, it can be concluded that the rate of diffusion to the surface is similar to the rate of drying, as the CRDP regime constitutes around 80% of the total drying period. The experimental result is similar to that reported for the drying of corncob and lotus rhizome.<sup>16,18</sup> The mathematical analysis of drying is generally represented by the  $D_{\text{eff}}$  calculated using eqn (2). It was observed that  $D_{\text{eff}}$  values increased with increasing microwave power.  $D_{\text{eff}}$  values of MWD dried star fruits were  $5.10 \times 10^{-8} \text{ m}^2 \text{ s}^{-1}$  at 100 W,  $8.01 \times 10^{-8} \text{ m}^2 \text{ s}^{-1}$  at 450 W and  $9.63 \times 10^{-8} \text{ m}^2 \text{ s}^{-1}$  at 800 W microwave power. Diffusivity values for HAD and FD samples were  $0.13 \times 10^{-8} \text{ m}^2 \text{ s}^{-1}$  and  $0.0563 \times 10^{-8} \text{ m}^2 \text{ s}^{-1}$  respectively. Therefore, 800 W microwave power has the highest value of moisture diffusivity and the FD sample has the lowest. The variation in the effective diffusivity value for different drying methods can be explained in terms of the physical processes involved in those techniques. The sublimation process is usually slower than other moisture removal processes due to greater energy requirements. For high temperature processes, an increase in vapour pressure and reduction in viscosity makes the escape of free water molecules from the



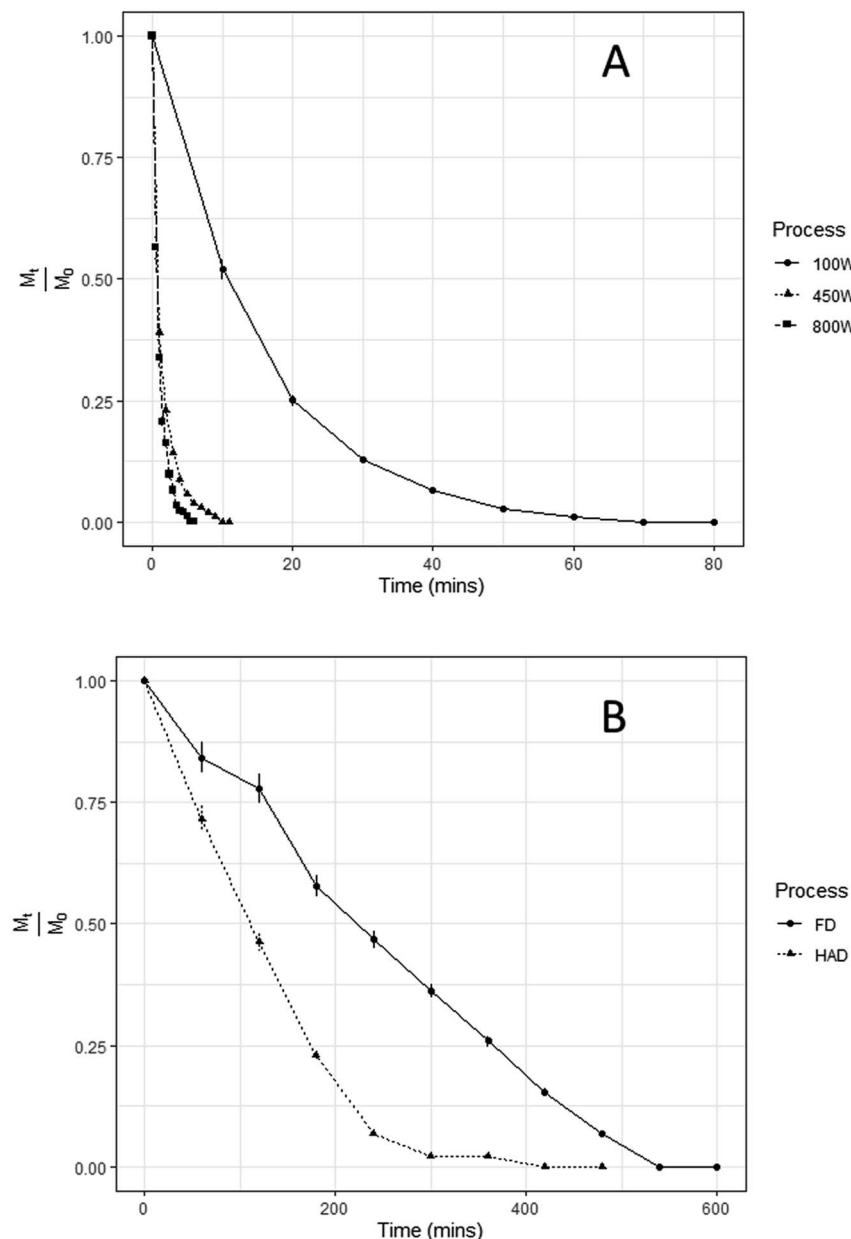


Fig. 1 (A) and (B) show the MR (moisture ratio) versus drying time of different methods of drying: MWD (microwave drying) 100 W, 450 W, and 800 W, HAD (hot air drying), and FD (freeze-drying).

cellular matrix easier. In microwave drying, the process is accelerated by the selective absorption of electromagnetic energy by water molecules *via* dipole rotation and ionic conduction. At higher microwave power, the process is further intensified by a more effective coupling between the energy, water and cellular material due to better dielectric properties, and higher water mobility and vapour pressure. The rapid increase in vapour pressure within the cells promotes rapid swelling and splitting of cells, which accelerated the moisture removal process.

MWD<sub>800W</sub> needed an average drying time of 26 minutes, whereas FD required a drying period of more than 10 hours (Table 2). The use of 800 W microwave drying reduced the time of drying by more than 80% when compared to 100 W and

enhanced moisture diffusivity by nearly two times. As a result, using microwave oven drying gives a significantly faster drying procedure with reduced energy usage and expense.

The thin layer models presuppose that throughout the whole drying process, the solid will have a uniform temperature and moisture distribution that matches the air-drying temperature. It is used to determine the drying time of food slices and to create drying curves.<sup>19</sup> MR *vs.* time (in s) data of dehydrated samples were fitted into seven distinct thin layer models eqn (6)–(12), and parameter estimates and error data for every model are presented in Tables 1 and 3. The results indicate an excellent correlation between actual and predicted values for all equations. (Table 4) Logarithmic and two-term



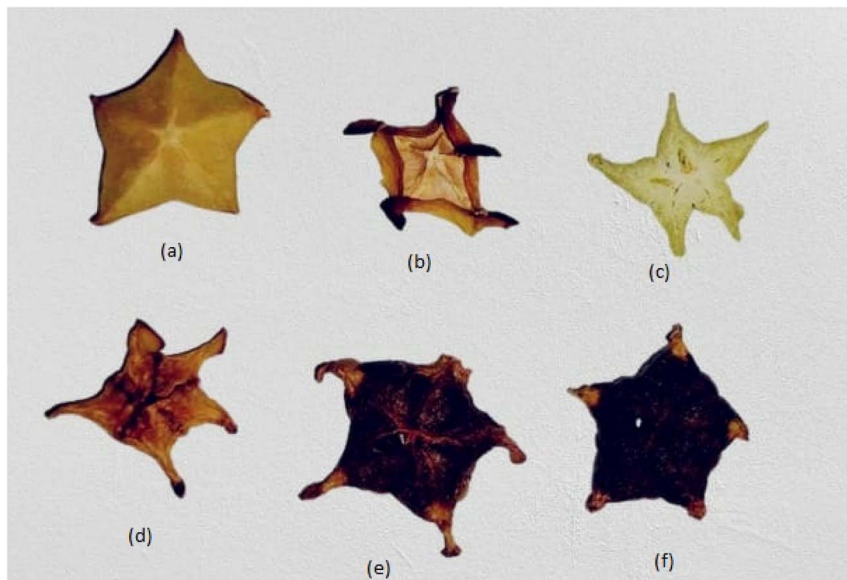


Fig. 2 Pictures of star fruit, (a) control, (b) HAD (hot air dried), (c) FD (freeze dried), (d) MWD 100 W (microwave dried at 100 W), (e) MWD 450 W (microwave dried at 450 W), and (f) MWD 800 W (microwave dried at 800 W).

Table 2 Drying time, calculated effective diffusivity value and hardness parameters for star-fruit before and after different methods of drying<sup>a</sup>

Sample	Time (min)	Effective diffusivity ( $10^{-8} \text{ m}^2 \text{ s}^{-1}$ )	Bulk density ( $\text{kg m}^{-3}$ )	Hardness (N)	Fracturability (N)	Adhesiveness	Resilience
Fresh	—	—	$655.43 \pm 0.15^{\text{a}}$	$19.99 \pm 0.02^{\text{a}}$	$3.70 \pm 0.02^{\text{a}}$	$25.96 \pm 0.58^{\text{a}}$	$0.01 \pm 0.00^{\text{a}}$
FD	600	0.06	$596.15 \pm 0.27^{\text{b}}$	$4.85 \pm 0.00^{\text{c}}$	$8.19 \pm 0.02^{\text{c}}$	$15.75 \pm 0.06^{\text{b}}$	$0.02 \pm 0.00^{\text{c}}$
HAD	480	0.13	$325.39 \pm 0.15^{\text{e}}$	$8.63 \pm 0.01^{\text{b}}$	$51.41 \pm 0.04^{\text{b}}$	$3.82 \pm 0.08^{\text{a}}$	$0.00 \pm 0.00^{\text{b}}$
MWD 100 W	60	5.1	$220.21 \pm 0.05^{\text{f}}$	$1.37 \pm 0.00^{\text{e}}$	$20.29 \pm 0.01^{\text{f}}$	$3.21 \pm 0.00^{\text{d}}$	$0.02 \pm 0.00^{\text{f}}$
MWD 450 W	11	8.01	$339.97 \pm 0.47^{\text{b}}$	$8.47 \pm 0.00^{\text{d}}$	$24.82 \pm 0.01^{\text{e}}$	$3.93 \pm 0.03^{\text{c}}$	$0.01 \pm 0.00^{\text{e}}$
MWD 800 W	5	9.63	$432.21 \pm 0.01^{\text{c}}$	$32.61 \pm 0.20^{\text{c}}$	$27.15 \pm 0.96^{\text{c}}$	$27.15 \pm 0.96^{\text{c}}$	$0.00 \pm 0.00^{\text{d}}$

<sup>a</sup> The superscripts a, b, c, d, e, and f in the same row show significant ( $p < 0.05$ ) values of structural and textural properties of star-fruits.  $\pm$  means the standard deviation (SD) of the sample. FD, freeze dried; HAD, hot air dried; MWD (microwave drying) 100 W, 450 W, and 800 W.

models are complex models having four and five constants, whereas Lewis, Page, Wang and Singh, Modified Page and Henderson Pabis models have one, two and three constants. The best appropriate model will be determined using statistical metrics that measure the model's predictability rather than the number of constants.<sup>20</sup> Among the equations above, the two-term model has the lowest SSE (0.000058–0.003581), RMSE (0.003742–0.021934) and reduced chi-square (0.000034–0.000583) value for every drying process, which indicates the suitability of the two-term model for analysing the drying of star fruits.

**Textural and structural characteristics.** The texture of a fruit depends on many parameters, especially the composition of the cell wall, relative amount of key constituents, maturation and water content, and can also be influenced by external factors such as economic, social, and cultural aspects.<sup>21</sup> By comparing the hardness, bulk density, and resilience of the product, the structural characteristics of star fruits and dried samples can be estimated. Fracturability describes the tendency of a food particle to fracture upon the application of a relatively small

amount of force or impact such as biting with the incisors.<sup>22</sup> Adhesiveness is a surface property of a material that causes it to stick to another material upon contact due to intermolecular attractive forces. Resilience refers to the ability of a food material to recover its original shape and size after being subjected to deformation. It is a measure of the elasticity and structural integrity of a food material.

Textural and structural characteristic results are shown in Table 2. Fruits with high water content like watermelon, star fruits, strawberries and peaches have soft and juicy textures characterized by low hardness and fracturability values. The presence of a large amount of water in fruit tissues makes it more amenable to deformation. The presence of water also allows the creation of a cohesive tissue structure by forming hydrogen bonds and improves structural integrity by maintaining the turgor pressure. Removal of water is associated with the creation of harder and more brittle dried products.<sup>23</sup> The maximum and minimum hardness values for MWD products were observed for 800 and 100 W, respectively. High temperature dried products, by HAD and MWD, have exhibited



**Table 3** Results of selected microwave, hot air, and freeze drying models' statistical analyses

(1) Lewis model: $MR = \exp(-k \times T)$			
Drying method	$k \times 10^3$		
MWD 800 W	17.22		
MWD 450 W	12.91		
MWD 100 W	1.14		
HAD	0.00016		
FD	0.11		

(2) Pages model: $MR = \exp(-kT^n)$			
Drying method	$k \times 10^6$	$n$	
MWD 800 W	40 800.12	0.75	
MWD 450 W	19 600	0.96	
MWD 100 W	485.18	1.12	
HAD	7.64	1.33	
FD	0.01	1.87	

(3) Modified pages model: $MR = \exp(-(kT)^n)$			
Drying method	$k \times 10^3$	$n$	
MWD 800 W	16.73	0.96	
MWD 450 W	13.72	0.75	
MWD 100 W	1.13	1.12	
HAD	0.19	1.33	
FD	0.12	1.87	

(4) Logarithmic model: $MR = a^* \exp(-k \times T) + c$			
Drying method	$k \times 10^3$	$a$	$c$
MWD 800 W	1078.10	0.97	0.02
MWD 450 W	865.30	0.95	0.04
MWD 100 W	1.11	1.01	-0.01
HAD	0.09	1.21	-0.19
FD	0.02	2.53	-1.53

(5) Henderson Pabis: $MR = a^* \exp(-k \times T)$			
Drying method	$k \times 10^3$	$a$	
MWD 800 W	17.00	0.98	
MWD 450 W	12.60	0.98	
MWD 100 W	1.14	1.00	
HAD	0.14	1.05	
FD	0.06	1.06	

(6) Two-term model: $MR = a^* \exp(-kT) + b^* \exp(-gT)$			
Drying method	$k \times 10^3$	$a$	$b$
MWD 800 W	15.21	0.88	0.12
MWD 450 W	8.17	0.63	0.37
MWD 100 W	1.19	1.06	-0.06
HAD	0.17	1.37	-0.37
FD	0.07	1.17	-0.17

(7) Wang and Singh model: $MR = 1 + aT + bT^2$			
Drying method	$a \times 10^6$	$b \times 10^9$	
MWD 800 W	-9744.35	22 606.90	
MWD 450 W	-5817.42	7825.71	
MWD 100 W	-731.98	131.2	
HAD	-95.15	2.31	
FD	-39.9783	0.3	

**Table 4** Goodness-of-fit analysis of seven different thin layer drying equations for different modes of drying of star-fruit<sup>a</sup>

Drying method	SSE $\times 10^3$	RMSE $\times 10^3$	Reduced chi-square $\times 10^3$
<b>Lewis model</b>			
MWD 800 W	3.69	19.22	0.33
MWD 450 W	12.00	36.47	1.33
MWD 100 W	0.26	6.63	0.04
HAD	27.20	67.32	4.53
FD	39.80	70.50	4.98
<b>Pages model</b>			
MWD 800 W	184.10	151.66	23.01
MWD 450 W	80.70	107.24	11.53
MWD 100 W	22.10	74.16	5.53
HAD	560.20	374.17	140.05
FD	99.50	128.84	16.58
<b>Modified pages model</b>			
MWD 800 W	184.10	151.66	23.01
MWD 450 W	80.70	107.24	11.53
MWD 100 W	22.10	74.36	5.53
HAD	560.20	374.30	140.05
FD	99.50	128.84	16.58
<b>Henderson pabis model</b>			
MWD 800 W	3.39	19.39	0.38
MWD 450 W	11.40	37.82	1.43
MWD 100 W	0.25	7.07	0.05
HAD	24.40	69.93	4.88
FD	33.40	69.14	4.77
<b>Logarithmic model</b>			
MWD 800 W	2.46	17.55	0.31
MWD 450 W	5.75	28.65	0.82
MWD 100 W	0.12	5.48	0.03
HAD	9.55	48.89	2.39
FD	3.68	24.78	0.61
<b>Two-term model</b>			
MWD 800 W	1.23	12.41	0.15
MWD 450 W	0.24	5.83	0.03
MWD 100 W	0.06	3.74	0.02
HAD	2.86	21.12	0.58
FD	3.58	21.93	0.51
<b>Wang and Singh model</b>			
MWD 800 W	92.30	101.30	10.26
MWD 450 W	172.11	147.00	21.51
MWD 100 W	20.90	64.70	4.18
HAD	2.96	24.30	0.59
FD	3.62	22.74	0.52

<sup>a</sup> MWD (microwave drying) 100 W, 450 W, and 800 W; HAD, hot air dried; FD, freeze dried; SSE, sum square error; RMSE, root mean square error.

significantly higher ( $p < 0.05$ ) fracturability and lower ( $p < 0.05$ ) adhesiveness and resilience values except for MWD<sub>800W</sub>. During the drying process, the removal of free water causes significant shrinkage in cellular volume and destruction of intermolecular H-bonds and lowers the turgor pressure of the tissue. Cell shrinkage is lowest in the FD samples, indicated by their bulk

density values. In freeze drying, the formation of ice crystals and consequent volume increase and puncture of the cell wall were responsible for the lower firmness of FD products.<sup>22</sup>

However, a gentle and lower thermal treatment at reduced pressure during FD produced the least variation in textural attributes. Additionally, intense drying at high temperature causes large-scale disintegration of the cellular structure.<sup>24</sup> All



Table 5 Comparison of Hunter color lab (CIELAB  $L^*$ ,  $a^*$  and  $b^*$ ) values of star-fruit before and after different methods of drying<sup>a</sup>

Parameters	Drying methods					
	control sample	HAD	FD	MWD 100 W	MWD 450 W	MWD 800 W
$L^*$	56.25 ± 0.01 <sup>b</sup>	40.51 ± 0.03 <sup>c</sup>	60.00 ± 0.01 <sup>a</sup>	31.47 ± 0.06 <sup>d</sup>	22.29 ± 0.04 <sup>e</sup>	21.51 ± 0.10 <sup>f</sup>
$a^*$	→6.40 ± 0.01 <sup>f</sup>	5.11 ± 0.02 <sup>e</sup>	8.84 ± 0.04 <sup>a</sup>	7.90 ± 0.14 <sup>b</sup>	6.80 ± 0.05 <sup>d</sup>	7.16 ± 0.03 <sup>c</sup>
$b^*$	32.06 ± 0.01 <sup>a</sup>	25.72 ± 0.03 <sup>c</sup>	28.07 ± 0.02 <sup>b</sup>	17.65 ± 0.05 <sup>d</sup>	9.20 ± 0.05 <sup>e</sup>	6.30 ± 0.05 <sup>f</sup>
$\Delta E$		20.51 ± 0.02 <sup>d</sup>	16.23 ± 0.03 <sup>e</sup>	30.05 ± 0.04 <sup>c</sup>	43.23 ± 0.03 <sup>b</sup>	45.24 ± 0.02 <sup>a</sup>
Chroma	32.67 ± 0.03 <sup>a</sup>	26.20 ± 0.05 <sup>c</sup>	29.45 ± 0.05 <sup>b</sup>	19.39 ± 0.04 <sup>d</sup>	11.44 ± 0.05 <sup>e</sup>	9.53 ± 0.05 <sup>f</sup>
Hue angle	101.20 ± 0.10 <sup>a</sup>	78.63 ± 0.15 <sup>b</sup>	72.43 ± 0.04 <sup>c</sup>	65.67 ± 0.07 <sup>d</sup>	53.46 ± 0.06 <sup>e</sup>	41.44 ± 0.05 <sup>f</sup>

<sup>a</sup> The superscripts a, b, c, d, e and f indicate the significant effect ( $p < 0.05$ ) and ± shows SD (standard deviation) of drying temperature. HAD, hot air dried; FD, freeze dried; MWD (microwave drying) 100 W, 450 W, and 800 W.

these factors are collectively responsible for the observed variation in the textural attributes of the dried star fruit samples.

**Color.** The most significant sensory attribute of a food product is its color, as it influences consumer perception and acceptance.<sup>25</sup> Visible color changes in dried products indicate the qualitative attributes of chemical changes that occurred during the process. Therefore, changes in bioactivity can be linked to the changes in the color of dried products.<sup>26</sup> For both control and dried star fruits, the color parameters ( $L^*$ ,  $a^*$ , and  $b^*$ ), the total color difference ( $\Delta E$ ), chroma ( $C^*$ ) and hue angle ( $H^*$ ) are shown in Table 5. The fresh star fruit has a mild darker color with a reddish-yellow hue due to the presence of cyanidin-3-*o*-glucoside and delphinidin-3-*o*-glucoside.<sup>27</sup> Drying induced color changes are associated with an increase in darkness due to the removal of water, the concentration of solids, degradation of pigments and formation of Maillard reaction products. Interestingly, FD products exhibited a higher  $L^*$  value (60.11) and similar  $a^*$  and  $b^*$  values. Freeze drying is often termed as the best drying technique for preserving the natural characteristics of the products. The removal of water makes the surface less opaque and lower shrinkage of cellular volume creates a porous sponge-like structure, both of which increase reflection of light from the surface of the material, and consequently,  $L$  values are increased. Da Silva *et al.* (2016)<sup>28</sup> reported a significant increase in the brightness value ( $L^*$ ) of melon and mangoes after drying. High temperature intense drying techniques, HAD and MWD star fruit samples exhibited lower  $L^*$ ,  $a^*$  and  $b^*$  values. Drying

at high temperatures caused significant degradation of thermo-stable anthocyanins, accelerating the Maillard reaction. Anthocyanin degradation products and Maillard reaction products have a darker color than their parent compounds, which is responsible for the significant darkening of dried products. These end products are also responsible for lower  $a^*$  and  $b^*$  values of HAD and MWD star fruits. A similar trend in results was described by Brar *et al.* (2020),<sup>29</sup> during the drying of yellow European plums, where they mentioned that drying at high temperatures developed darker color products. The results presented in this work suggested that FD and HAD can better preserve the anthocyanin content and color of star fruit than the microwave drying technique. This result is similar to color changes observed in okra during drying.<sup>30</sup> The best quality dried samples should have the color closest to the original color of the fresh sample. The highest  $\Delta E$  value was obtained for the MWD 800 W sample. The magnitude of color change  $\Delta E$  increases with microwave power ( $\Delta E$ : 31–44 at 100–800 W). The FD and HAD samples had shown a lower total color difference value than the MWD samples. The results presented in this work suggested that FD and HAD can better preserve the color of star fruits than the microwave drying method.

**TPC and TFC.** An optimum drying technique is a critical post-harvest processing method since it enables extending the shelf life of perishable goods and preserves important bioactive components of the sample. Generally, dried fruits and vegetables have lower antioxidant content than their fresh

Table 6 TPC, TFC and antioxidant values of different drying methods<sup>a</sup>

Drying methods	TPC mg GAE/100 g	TFC mg QE/100 g	FRAP $\mu\text{mol g}^{-1}$	DPPH inhibition (%)
Control	1810.67 ± 1.66 <sup>a</sup>	21.54 ± 0.18 <sup>a</sup>	847.12 ± 1.73 <sup>a</sup>	97.19 ± 0.15 <sup>a</sup>
HAD	1139.67 ± 4.07 <sup>b</sup>	4.71 ± 0.05 <sup>b</sup>	148.52 ± 0.05 <sup>b</sup>	95.67 ± 0.6 <sup>b</sup>
FD	876.17 ± 6.5 <sup>d</sup>	3.83 ± 0.25 <sup>c</sup>	119.20 ± 0.39 <sup>d</sup>	91.3 ± 0.27 <sup>c</sup>
MWD 100 W	969.17 ± 1.04 <sup>c</sup>	2.99 ± 0.10 <sup>d</sup>	118.50 ± 0.5 <sup>d</sup>	84.87 ± 0.4 <sup>e</sup>
MWD 450 W	970.27 ± 2.8 <sup>c</sup>	3.41 ± 0.01 <sup>c</sup>	129.70 ± 0.35 <sup>c</sup>	89.30 ± 0.32 <sup>d</sup>
MWD 800 W	790.13 ± 7.7 <sup>d</sup>	2.88 ± 0.11 <sup>d</sup>	84.58 ± 0.52 <sup>e</sup>	76.94 ± 0.50 <sup>f</sup>

<sup>a</sup> Values are presented as mean ± standard deviation of triplicate experiments. Means that do not share a letter are significantly different ( $p < 0.05$ ). GAE means gallic acid equivalent, QE means quercetin equivalent. TPC, total phenolic content; TFC, total flavonoid content; FRAP, ferric reducing antioxidant potential; DPPH, (2, 2-diphenyl-1-picrylhydrazyl) radical scavenging activity; HAD, hot air dried; FD, freeze dried; MWD (microwave drying) 100 W, 450 W, and 800 W.



counterparts owing to thermal degradation and disintegration of key thermo-labile antioxidants at high temperature.<sup>31</sup> However, cellular disintegration and depolymerisation of bound complexes, which primarily remain bound to oligo and poly-saccharides *via* glycosidic bonds, can release previously unavailable phenolics that possess antioxidant activity, which will then increase the antioxidant content after drying.<sup>32,33</sup> Enzymes like peroxidase can also degrade available phenolic compounds in fresh samples and lower the antioxidant content. Therefore, the deactivation of the peroxidase enzyme during drying will stabilize the antioxidant content.<sup>31</sup> One of the key aims of this research was to investigate the effect of different modes of drying on the anti-oxidant activity of star fruits. The TPC and TFC value of fresh samples were  $1810.67 \pm 1.66$  mg GAE/100 g dm and  $21.54 \pm 0.18$  mg QE/100 g dm, respectively (Table 6). The previously reported value of the fresh star fruit juice antioxidant content is  $540.80 \pm 16.64$  mg GAE/100 ml which is lower than that found in this study.<sup>34</sup> This variance in the total phenolic content was discovered as a result of the various environmental factors, cultivar varieties, and soil conditions.

According to research, the phenolic content of star fruit juice might change based on the temperature and reaction time. Shourove *et al.* (2020)<sup>34</sup> studied fruit juice at various treatment temperatures (70 °C, 80 °C, and 90 °C). High TPC content was found in the control sample (540 mg GAE/100 ml) followed by drying at HAD (443 mg GAE/100 g). In this study, among the thermally treated samples, the highest TPC and TFC values of 1139.67 mg GAE/100 g dm and 4.71 mg QE/100 g were reported for HAD samples. Among MWD samples, the 450 W MWD star fruit samples exhibited the highest TPC value of 970.27 mg GAE/100 g dm and TFC value of 3.41 mg QE/100 g dm. Microwave drying from 800 W to 100 W reduced the TPC significantly from 969.17 to 790.13 mg GAE/100 g dm.

Oxidation of phenolic compounds during a prolonged drying period and accelerated degradation of thermolabile compounds caused by intense heating at high temperatures were responsible for the observed variation in the antioxidant content of dried star fruit samples.

Kondareddy *et al.* (2020)<sup>35</sup> studied the variation of the phenolic content of fresh and dried fruits under different conditions. The TPC of a fresh sample was  $5.88 \pm 0.27$  mg g<sup>-1</sup> while the solar dried sample's TPC was found to be  $8.11 \pm 0.15$  mg g<sup>-1</sup>. V. T. Nguyen *et al.* (2015)<sup>36</sup> reported similar results for *Phyllanthus amarus* drying. Samples subjected to hot air drying at 70 °C exhibited 15–30% higher TPC values than those subjected to other drying processes. For drying of mung bean and *Stevia rebaudiana* leaves, authors attributed the higher TPC of HAD products than FD products to the faster drying time and higher temperature, which helped to preserve the phenolic compounds and minimize oxidative degradation.<sup>37,38</sup> For the drying of star fruits, the higher TPC content of HAD star fruits might be a result of such factors.

TFC values of dried star fruit decreased in the given order: HAD > FD > MWD<sub>450</sub> > MWD<sub>100</sub> > MWD<sub>800</sub> (Table 6). The highest TFC content was recorded for HAD (4.71 mg QE/100 g) samples. During drying at high temperature, bound phenolic

compounds were released through non-enzymatic interconversion by rupturing the cell wall. The higher amount of TFC was primarily involved with increased enzyme activity (phenylalanine ammonia-lyase).<sup>39</sup> No statistically significant ( $p < 0.05$ ) difference was observed between MWD<sub>450</sub> – MWD<sub>800</sub> and FD – MWD<sub>100</sub> samples. Flavonoids, especially flavonol, flavone and anthocyanin, are principally responsible for reducing the antioxidant activity of star fruits. These compounds are most stable at temperatures below 60 °C and disintegrate rapidly as the temperature is gradually increased. Brief exposure to high temperatures and intense heating is sufficient to cause a significant reduction in flavonoid content. Flavonoids such as anthocyanins are extremely heat-sensitive and can rapidly disintegrate after a brief exposure to intense heating. Both during high power MW drying (800 MWD) and prolonged heating at relatively lower power (100 MWD), lower values of TFC were reported at 2.88 mg QE/100 g dm for 800 W and 2.99 mg QE/100 g for 100 W respectively.

Compared to microwave drying, the heating intensity and process temperature are lower during freeze and oven drying, thereby showing a lower loss of flavonoids. Samples dried by HAD had a higher TFC content than FD samples.

It was observed that the loss of flavonoid content in dried star fruit is more severe than phenolic content loss. In dried star fruit samples, the loss of flavonoid content was between 79 and 88%, far higher than the 38–54% loss reported for total phenolic content. Therefore, it can be inferred that non-flavonoid phenolic compounds present in star fruits have better thermal stability than flavonoids. It should also be noted that in the color section, we showed that significant color differences after high-temperature drying might be a result of the degradation of key anthocyanin pigments. A similar difference between phenolic and flavonoid stability was reported for the drying of stevia leaves.<sup>37</sup>

#### Determination of radical scavenging activity (DPPH) and ferric reducing activity power (FRAP)

Antioxidant activity assays are generally classified into two distinct categories: hydrogen atom transfer (HAT) and electron transfer (ET) based.<sup>40</sup> DPPH radical scavenging assay assesses the capacity of the antioxidant to donate an H atom to the DPPH radical. A solvent like methanol was used for the extraction of different treated dried powders. After an incubation of 90 minutes, DPPH radical scavenging activity was determined spectrophotometrically. FRAP assay is an ET-based method that determines antioxidant power based on reduction at low pH of a ferric complex ( $\text{Fe}^{3+}$ ) to a ferrous complex ( $\text{Fe}^{2+}$ ).<sup>41</sup> Color change of the dried star fruit methanolic extract and antioxidants of the control was tested. HAD samples showed the highest FRAP activity and DPPH radical scavenging activity (Table 6). Although FD is often considered the best method for preserving nutrients, the results presented in this study showed that hot air drying produced a better end product in terms of antioxidant content. FRAP activity of dried star fruits increased in the following order: MWD<sub>800</sub> < MWD<sub>100</sub> < FD < MWD<sub>450</sub> < HAD, whereas DPPH activity increased in the order: MWD<sub>800</sub> <



$MWD_{100} < MWD_{450} < FD < HAD$ . All microwave dried samples exhibited a far lower antioxidant activity, with  $MWD_{800}$  being the worst and  $MWD_{450}$  the best. Coffee<sup>42</sup> and mango seed kernel flour have both shown improved antioxidant activity with high temperatures.<sup>43,44</sup>

The antioxidant value of star fruits denotes the medicinal and nutraceutical potential. From the values presented in Table 6 and it is evident that the fresh sample has the highest antioxidant activity due to its higher phenolic and flavonoid content. The variation in DPPH radical scavenging activity (3–23% reduction) is lower than in FRAP activity (82.5–90% reduction). This observed variation in antioxidant activities can be attributed to various factors. First, the reduction of flavonoid content after drying was similar to that of FRAP, and therefore, it can be assumed that flavonoids in star fruits act primarily as a reducer by electron transfer. The presence of polar functional groups such as hydroxyl and carbonyl groups that act as electron donors and higher solubility in polar solvents (*i.e.* water, methanol) may contribute to the higher FRAP activity of flavonoids.<sup>45</sup> Second, various other non-phenolic non-flavonoid compounds such as carotenoid, tocopherol and ascorbic acid, as well as a few amino acids like proline, histidine and selective minerals (Se and Zn), can contribute to the DPPH and radical scavenging activity. Their contribution to the activity may depend on their concentration, chemical structure and assay condition.<sup>46</sup>

They are also more thermo-stable than flavonoids. From the analysis of the antioxidant content-activity value, it is evident

that non-flavonoid phenolic compounds and non-phenolic non-flavonoid compounds are principally responsible for the strong DPPH radical scavenging activity of dried star fruits.

**HPLC assay.** High-performance liquid chromatography (HPLC) is an effective method for the identification and measurement of bioactive components. The phenolic compounds quantified were ascorbic acid, picomeric acid, dihydroxybenzoic acid, catechin, caffeic acid, chlorogenic acid, vanillic acid, rutin, elachic acid, sinapic acid, tannic acid, *trans*-cinnamic acid, myricetin, apigenin, and kaempferol. Among all phenolic compounds (ESI Fig. S1†) identified in extracts of the control sample, the most significant variation was noticed in the case of rutin. The most prevalent phenolic compounds in dried star fruit were chlorogenic acid and *trans*-cinnamic acid.

In the 450 W MWD sample and HAD sample,  $177.89 \pm 5.33$  mg/100 g dm and  $186.85 \pm 5.60$  mg/100 g of *trans*-cinnamic acid were present, respectively, and significant changes were found ( $p < 0.05$ ). *trans*-Cinnamic acid content was increased with the varied intensity of drying. The content of gallic acid, chlorogenic acid and myracitine was significantly decreased at a high microwave power level and longer exposure time (Fig. 3). Kaempferol was the heat sensible and unstable polyphenol compared to others because it significantly increases with increasing temperature of HAD and  $MWD_{450W}$  but decreased for  $MWD_{100W}$  and  $MWD_{800W}$ . In this study, control star fruits contain  $43.35 \pm 1.30$  mg/100 g kaempferol while  $MWD_{800}$  contains  $37.23 \pm 1.11$  mg/100 g. In this study compared to the control, *trans*-cinnamic acid increased by almost 28% and 22%

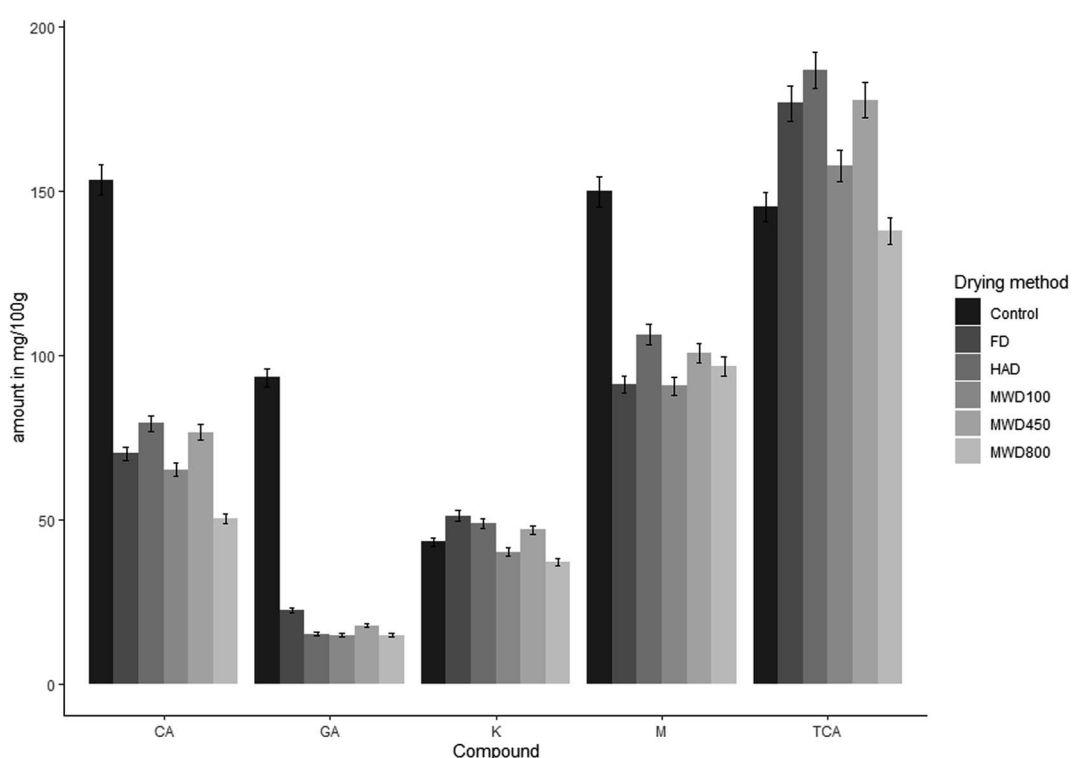


Fig. 3 HPLC chromatogram graph of star fruit. Hare CA (chlorogenic acid), GA (gallic acid), K (kaempferol), M (myracitine), and TAC (*trans*-cinnamic acid). Control, (fresh sample); FD, (freeze dried); HAD, (hot air dried); MWD 100, (microwave dried at 100 W); MWD 450, (microwave dried at 450 W); MWD 800, (microwave dried at 800 W).



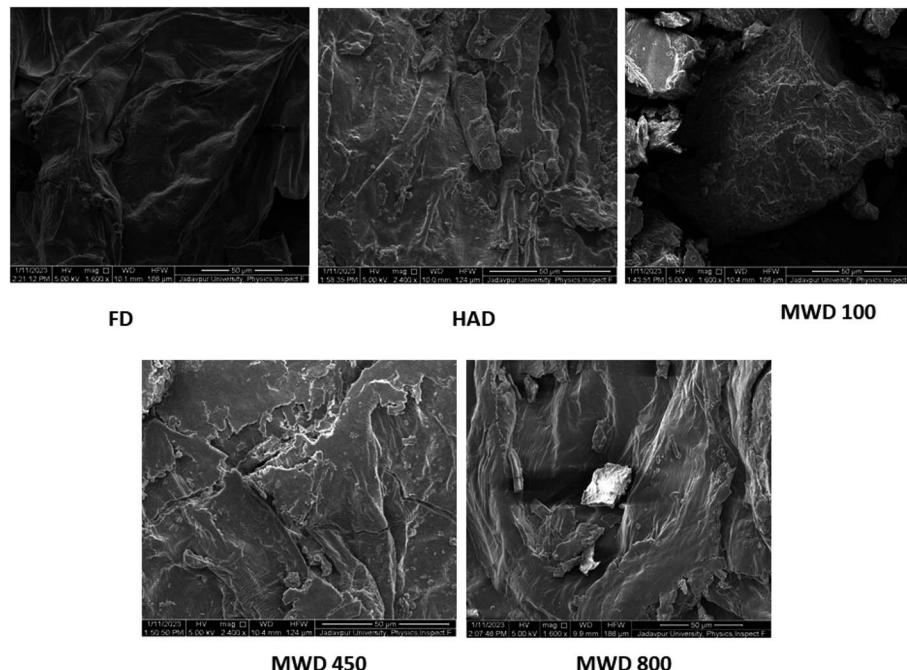


Fig. 4 SEM images of dried powder star fruits. FD – freeze dried, HAD-hot air dried, MWD 100 – microwave dried at 100 W, MWD 450 – microwave dried at 450 W, and MWD 800 – microwave dried at 800 W.

for HAD and MWD<sub>450W</sub> respectively. The results are also similar to the antioxidant properties of dried tomatoes.<sup>47</sup>

#### Effect of drying on the star fruit's microstructure

The SEM images of different star fruit dried powder samples are presented in Fig. 4 to illustrate drying induced changes in the microstructure of the sample. As can be seen in Fig. 4, the drying temperature had the greatest impact on the star fruit tissue structure, leading to damaged cell walls and ruptured cellular membranes in numerous places and formation irregular shapes and also shrinkage of the cell wall. The principal changes in fruit tissue during drying can be summarized into three different types:

- Cracks and fissures
- Surface roughness
- Structural changes

The rapid increase in vapour pressure within the cell during drying and shrinkage after water removal causes internal stresses in the cell structure and alters the surface tension, leading to the formation of cracks, fissures, bumps, ridges or pores. All of these changes are indicative of intense drying and rapid removal of water at high temperature, which created a large amount of stress in the cellular structure that exceeds the natural capacity of the fruit tissue. In oven drying, cell rupturing and destruction were higher than in FD star fruit. In microwave drying, the cell structure was fully destructed and ruptured due to sudden temperature increases *via* electromagnetic waves and also internal pressure increases due to high vapour pressure. The extent of degradation was increased with increasing microwave power. These physical processes are also responsible for the development of hard and brittle structures

with low resilience and adhesiveness after high-temperature drying. The scientists found similar results for the microstructure of dried ginger, bamboo shoots, and Chrysanthemum flowers, in that order.<sup>48</sup>

In contrast, the surface of the freeze-dried sample exhibited a smooth, granular, porous and minimally shrunken cell structure. It has maintained its original form. The formation of ice crystals during freezing causes the cell material to expand. Sublimation at low temperatures and pressure preserves the original structure and composition and generates a granular and porous structure. Low processing temperature and pressure greatly lowers physical stresses and limit structural changes. This is also in line with lower bulk density or higher product volume and better textural attribute values for FD samples.

#### Conclusion

This research work investigated the effect of different methods of drying on various qualitative and quantitative attributes of star fruits. Microwave drying shortens the required processing time and greatly reduces the energy requirement than both freeze and hot air drying. Among seven different thin layer drying models evaluated in this study, a two-term model was found to be best for analysing the drying curve for star fruits with the lowest SSE, RMSE and reduced chi-square value. The FD sample exhibited the least deviation in textural and color attributes from the control sample, as a low temperature and pressure gradient maintained the smooth, granular and porous structure of fresh fruits. In contrast, high temperature dried star fruits demonstrated a hard and brittle structure with low resilience and adhesiveness due to the fast moisture removal



process and high pressure gradient during drying. High temperature dried products also exhibited the darker color characteristic of phenolic degradation products than the FD sample. The FD sample showed the least deviation in terms of perceivable color change from the fresh samples. Among all dried samples, HAD star fruit had the highest phenolic ( $1139.67 \pm 4.07$  mg GAE/100 g) and flavonoid ( $4.71 \pm 0.05$  mg QE/100 g) content, DPPH radical scavenging activity ( $95.67 \pm 0.6\%$ ) and FRAP ( $148.52 \pm 0.05 \mu\text{mol g}^{-1}$ ) activity. Among microwave dried samples, 450 W produced the best product in terms of textural, color and antioxidant attributes. Higher and lower microwave power accelerated thermal and oxidative degradation of key cellular constituents, leading to a product with lower quality attributes. Dried star fruit with a rich content of phenolic compounds and strong antioxidant activity can serve as an excellent source of bioactive raw material that can be effectively utilized in different industries such as food, nutraceutical, pharmaceutical and cosmetics. Future studies can be performed on the extraction of bioactive compounds from star fruits using a combination of drying methods like non-thermal pre-treatment followed by HAD.

## Author contributions

Jayanti Dhara: conceptualization, research methodology, experimentation, data analysis, manuscript writing—original draft. Suman Kumar Saha: research methodology, manuscript editing. Madhumita Saha: experimentation data analysis. Runu Chakraborty: supervision, conceptualization, project funding acquisition, resource generation, administration, validations, manuscript review and editing.

## Conflicts of interest

There are no conflicts to declare.

## References

- Y. Lu, C. W. Tan, D. Chen and S. Q. Liu, *Food Sci. Nutr.*, 2018, **6**, 2141–2150.
- K. A. Yuliadhi, I. W. Susila, I. W. Supartha, A. Sultan, I. K. W. Yudha, I. W. E. K. Utama and P. A. Wiradana, *IOP Conf. Ser.: Earth Environ. Sci.*, 2022, **980**, 012051.
- F. Salim, N. Adnan, N. S. Shuib and R. Mohd Yusof, *Jurnal Intelek*, 2022, **17**, 55.
- H. E. Khoo, A. Azlan, K. W. Kong and A. Ismail, *J. Evidence-Based Complementary Altern. Med.*, 2016, 1–20.
- R. Pliego-Arreaga, C. Regalado, A. Amaro-Reyes and B. E. García-Almendárez, *Rev. Mex. Ing. Quím.*, 2013, **12**, 505–511.
- R. N. Pereira and A. A. Vicente, *Food Res. Int.*, 2010, **43**, 1936–1943.
- F. Chemat, M. Abert Vian, A. S. Fabiano-Tixier, M. Nutrizio, A. Režek Jambrak, P. E. S. Munekata, J. M. Lorenzo, F. J. Barba, A. Binello and G. Cravotto, *Green Chem.*, 2020, **22**, 2325–2353.
- A. Hazervazifeh, P. A. Moghaddam and A. M. Nikbakht, *J. Food Process Eng.*, 2017, **40**, 1–10.
- Y. Liu, Y. Zhao and X. Feng, *Appl. Therm. Eng.*, 2008, **28**, 675–690.
- M. M. Özcan, F. Al Juhami, I. A. M. Ahmed, N. Uslu, E. E. Babiker and K. Ghafoor, *J. Food Sci. Technol.*, 2020, **57**, 233–242.
- T. V. L. Nguyen, M. D. Nguyen, D. C. Nguyen, L. G. Bach and T. D. Lam, *Processes*, 2019, **7**, 21.
- N. M. Shofian, A. A. Hamid, A. Osman, N. Saari, F. Anwar, M. S. P. Dek and M. R. Hairuddin, *Int. J. Mol. Sci.*, 2011, **12**, 4678–4692.
- S. Ray, S. K. Saha, U. Raychaudhuri and R. Chakraborty, *J. Food Meas. Charact.*, 2017, **11**, 639–650.
- C. J. Ridgway and P. A. C. Gane, *Nord. Pulp Pap. Res. J.*, 2003, **18**, 24–31.
- T. Sarkar, M. Salauddin, S. Pati, H. I. Sheikh and R. Chakraborty, *J. Food Process. Preserv.*, 2021, **45**, 1–20.
- S. K. Saha, S. Dey and R. Chakraborty, *J. Food Process Eng.*, 2019, **42**, 1–13.
- M. Suriya, G. Baranwal, M. Bashir, C. K. Reddy and S. Haripriya, *LWT–Food Sci. Technol.*, 2016, **68**, 235–243.
- Z. Z. Qiu and K. B. Chin, *Int. J. Food Sci. Technol.*, 2022, **57**, 2393–2401.
- N. S. Md Salim, Y. Gariépy and V. Raghavan, *J. Food Process. Preserv.*, 2017, **41**, e12905.
- D. I. Onwude, N. Hashim, R. B. Janius, N. M. Nawi and K. Abdan, *Compr. Rev. Food Sci. Food Saf.*, 2016, **15**, 599–618.
- S. Mounir, C. Téllez-Pérez, K. V. Sunooj and K. Allaf, *J. Texture Stud.*, 2020, **51**, 276–289.
- A. M. Paula and A. C. Conti-Silva, *J. Food Eng.*, 2014, **121**, 9–14.
- K. Ranganathan, V. Subramanian and N. Shanmugam, *Crit. Rev. Food Sci. Nutr.*, 2016, **56**, 2665–2694.
- A. Vega-Gálvez, K. Ah-Hen, M. Chacana, J. Vergara, J. Martínez-Monzó, P. García-Segovia, R. Lemus-Mondaca and K. Di Scala, *Food Chem.*, 2012, **132**, 51–59.
- M. Maskan, *J. Food Eng.*, 2001, **48**, 177–182.
- V. Sant'Anna, P. D. Gurak, L. D. Ferreira Marczak and I. C. Tessaro, *Dyes Pigm.*, 2013, **98**, 601–608.
- A. Ana Cristina, M. S. Gouvêa, A. Melo, M. C. P. A. Santiago, F. M. Peixoto, V. Freitas, R. L. O. Godoy and I. M. P. L. V. O. Ferreira, *Food Chem.*, 2015, **185**, 277–283.
- G. Dias da Silva, Z. M. P. Barros, R. A. B. de Medeiros, C. B. O. de Carvalho, S. C. Rupert Brandão and P. M. Azoubel, *LWT–Food Sci. Technol.*, 2016, **74**, 114–119.
- H. S. Brar, P. Kaur, J. Subramanian, G. R. Nair and A. Singh, *International Journal of Fruit Science*, 2020, **20**, S252–S279.
- I. Taruna and J. Astuti, *IOP Conf. Ser.: Earth Environ. Sci.*, 2018, **131**, 012007.
- J. Pinela, L. Barros, M. Dueñas, A. M. Carvalho, C. Santos-Buelga and I. C. F. R. Ferreira, *Food Chem.*, 2012, **135**, 1028–1035.
- S. Roshanak, M. Rahimmalek and S. A. H. Goli, *J. Food Sci. Technol.*, 2016, **53**, 721–729.
- I. D. Boateng and X. M. Yang, *J. Sci. Food Agric.*, 2021, **101**, 3290–3297.



34 J. H. Shourove, W. Zzaman, R. S. Chowdhury and M. M. Hoque, *Asian J. Agric. Food Sci.*, 2020, 41–53.

35 R. Kondareddy, N. Sivakumaran, K. Radhakrishnan and P. K. Nayak, *IOP Conf. Ser.: Earth Environ. Sci.*, 2020, **463**, 012138.

36 V. T. Nguyen, Q. V. Vuong, M. C. Bowyer, I. A. V. Altena and C. J. Scarlett, *Drying Technol.*, 2015, **33**, 1006–1017.

37 A. Periche, M. L. Castelló, A. Heredia and I. Escriche, *Food Chem.*, 2015, **172**, 1–6.

38 R. Y. Gan, W. Y. Lui, C. L. Chan and H. Corke, *J. Food Process. Preserv.*, 2017, **41**, 2–9.

39 A. Kheto, S. Dhua, P. K. Nema and V. S. Sharanagat, *J. Food Process Eng.*, 2021, **44**, 13880.

40 V. H. Borda-Yepes, F. Chejne, L. V. Daza-Olivella, A. F. Alzate-Arbelaez, B. A. Rojano and V. G. S. Raghavan, *J. Food Process Eng.*, 2019, **42**, 1–10.

41 K. Kogure, S. Goto, M. Nishimura, M. Yasumoto, K. Abe, C. Ohiwa, H. Sassa, T. Kusumi and H. Terada, *Biochim. Biophys. Acta, Gen. Subj.*, 2002, **1573**, 84–92.

42 I. Sánchez-González, A. Jiménez-Escríg and F. Saura-Calixto, *Food Chem.*, 2005, **90**, 133–139.

43 S. Zia, M. R. Khan and R. M. Aadil, *J. Food Meas. Charact.*, 2023, **17**, 1068–1081.

44 S. D. Subramaniam, N. B. Muhammad and L. A. Halim, *Mater. Today: Proc.*, 2023, 1–14.

45 Y. Zhang, Y. Li, X. Ren, X. Zhang, Z. Wu and L. Liu, *Food Chem.*, 2023, **402**, 134231.

46 P. Neupane and J. Lamichhane, *Vegetos*, 2020, **33**, 360–366.

47 C. H. Chang, H. Y. Lin, C. Y. Chang and Y. C. Liu, *J. Food Eng.*, 2006, **77**, 478–485.

48 R. Lemus-Mondaca, L. Zura-Bravo, K. Ah-Hen and K. Di Scala, *J. Sci. Food Agric.*, 2021, **101**, 6484–6495.

49 B. W. K. Lewis, *J. Ind. Eng. Chem.*, 1921, **13**, 427–432.

50 İ. Doymaz and O. İsmail, *Food Bioprod. Process.*, 2011, **89**, 31–38.

51 L. M. Diamante and P. A. Munro, *Sol. Energy*, 1993, **51**, 271–276.

52 *Proceedings of the 7th International Congress on Agricultural Mechanization and Energy*, ed. F. C. A. Yagcioglu, A. Degirmencioglu and A. Bascetincelik, Adana, Turkey.

53 S. M. Henderson and S. Pabis, *J. Agric. Econ.*, 1962, **7**, 85–89.

54 A. V. Prabhudesai and C. V. Viswanathan, *Chem. Phys. Lipids*, 1978, **22**, 71–77.

55 J. F. Steffe and R. P. Singh, *Trans. ASAE*, 1980, **23**, 767–0774.

